Received: 10 July 2018 | Revised: 21 March 2019 | Accepted: 9 April 2019

DOI: 10.1111/bph.14695

RESEARCH PAPER

Inhibitors of DAG metabolism suppress CCR2 signalling in human monocytes

Priscilla Day | Lisa Burrows | David Richards | Samuel J. Fountain

Biomedical Research Centre, School of Biological Sciences, University of East Anglia, Norwich, UK

Correspondence
Samuel J. Fountain, Biomedical Research Centre, School of Biological Sciences, University of East Anglia, Norwich NR4 7TJ, UK.
Email: s.j.fountain@uea.ac.uk

Funding information
British Heart Foundation, Grant/Award Number: PG/16/94/32393

Background and Purpose: CCL2 is an inflammatory chemokine that stimulates the recruitment of monocytes into tissue via activation of the GPCR CCR2.

Experimental Approach: Freshly isolated human monocytes and THP-1 cells were used. Fura-2 loaded cells were used to measure intracellular Ca^{2+} responses. Transwell migration to measure chemotaxis. siRNA-mediated gene knock-down was used to support pharmacological approaches.

Key Results: CCL2 evoked intracellular Ca^{2+} signals and stimulated migration in THP-1 monocytic cells and human $CD14^{+}$ monocytes in a CCR2-dependent fashion. Attenuation of DAG catabolism in monocytes by inhibiting DAG kinase (R59949) or DAG lipase (RHC80267) activity suppressed CCL2-evoked Ca^{2+} signalling and transwell migration in monocytes. These effects were not due to a reduction in the number of cell surface CCR2. The effect of inhibiting DAG kinase or DAG lipase could be mimicked by addition of the DAG analogue 1-oleoyl-2-acetyl-sn-glycerol (OAG) but was not rescued by application of exogenous phosphatidylinositol 4,5-bisphosphate. Suppressive effects of R59949, RHC80267, and OAG were partially or fully reversed by Gö6983 (pan PKC isoenzyme inhibitor) but not by Gö6976 (PKCα and PKCβ inhibitor). RNAi-mediated knock-down of DAG kinase α isoenzyme modulated CCL2-evoked Ca^{2+} responses in THP-1 cells.

Conclusions and Implications: Taken together, these data suggest that DAG production resulting from CCR2 activation is metabolised by both DAG kinase and DAG lipase pathways in monocytes and that pharmacological inhibition of DAG catabolism or application suppresses signalling on the CCL2–CCR2 axis via a mechanism dependent upon a PKC isoenzyme that is sensitive to Gö6983 but not Gö6976.

1 | INTRODUCTION

Chemokines are low MW extracellular signalling peptides secreted by tissue either constitutively during homeostasis or de novo during an inflammatory response (Griffith, Sokol, & Luster, 2014). They are a diverse family of peptides (CC, CXC, CX_3C, and XC chemokines) with a key role in the tissue recruitment and interstitial migration of leukocytes and other cell types, as well as acting both as chemoattractants and as cues for cellular arrest (Alon & Feigelson, 2012; Serbina & Pamer, 2006). The biological affects of chemokines are exerted through the activation of GPCRs expressed on the cell surface of target cells. In addition to beneficial roles in homeostasis and immunity (Luther et al., 2002), the activity of chemokines is also associated with the onset and progression of chronic inflammatory diseases including atherosclerosis and rheumatoid arthritis (Zernecke & Weber, 2010). To this end, several drug discovery programmes have been initiated in an effort to pharmacologically intervene in chemokine receptor signalling for therapeutic benefit. Targeting single chemokine receptors has proven to be difficult to translating to clinical efficiency, likely due to a level of redundancy between chemokine receptor subtypes. Dual therapy has been proposed as a strategy to overcome this, in addition to targeting convergent second messenger pathways (Horuk, 2009).

Abbreviations: CCL2, monocyte chemoattractant protein 1/chemokine ligand 2; PBMCs, peripheral blood mononuclear cells

The chemokine **CCL2** (monocyte chemoattractant protein-1; MCP-1) activates **CCR2**, a G_i-coupled GPCR that elevates intracellular Ca^{2+} responses and inhibits adenylate cyclase activity (Campwala, Sexton, Crossman, & Fountain, 2014). Classical $CD14^+/CD16^-$ blood monocytes express high levels of cell surface CCR2 (Weber et al., 2000), in comparison to nonclassical $CD14^+/CD16^+$ monocytes. In animal models of atherosclerosis, it has been demonstrated that CCL2 signalling via CCR2 plays an important role in the size of monocyte/macrophage vascular wall infiltrate and size of atherosclerotic lesion (Boring, Gosling, Cleary, & Charo, 1998; Gu et al., 1998; Lutgens et al., 2005; Veillard et al., 2005). CCL2 is also presented on the cell surface of vascular endothelium and participates in monocyte recruitment by stimulating firm adhesion and transmigration to the subendothelial space (Ashida, Arai, Yamasaki, & Kita, 2001; Maus et al., 2002; Wang et al., 1995). The importance of CCL2–CCR2 signalling does not match by our understanding of the signal transduction mechanisms that regulate functional responses in human monocytes (Cronshaw, Owen, Brown, & Ward, 2004; Webb et al., 2008).

Chemokines including CCL2 elicit intracellular Ca^{2+} responses in leukocytes and other cell types (Campwala et al., 2014; Korniejewska, McKnight, Johnson, Watson, & Ward, 2011). The responses are pertussis toxin-sensitive and dependent upon **PLC** (Campwala et al., 2014). The involvement of PLC suggests that DAG would be generated during generation of CCL2-evoked Ca^{2+} responses. DAG is a second messenger in its own right and can modulate the activity of PKC and several ion channels. Once produced by cells, DAG is rapidly metabolised by two major pathways: (a) conversion to phosphatidic acid by DAG kinase and (b) hydrolysis to free fatty acid and monoacylglycerol by **DAG lipase** (Reisenberg, Singh, Williams, & Doherty, 2012). The aim of this study was to investigate the role of DAG metabolising enzymes on CCL2-evoked intracellular Ca^{2+} responses and cellular function in human monocytes.

What is already known

- CCL2-mediated monocyte recruitment to tissue is involved in the onset and development of several chronic inflammatory diseases.

What this study adds

- Pharmacological inhibition of DAG metabolism is a novel route to attenuate CCL2 signalling in human monocytes.

What is the clinical significance

- Possible therapeutic route in inflammatory diseases with sustained monocyte tissue recruitment.

2 | METHODS

2.1 | Isolation of $CD14^+$ monocyte from human peripheral blood

All work was undertaken with the approval of the Faculty of Medicine and Health Sciences Research Ethics Committee, University of East Anglia, and NHS Health Research Authority Ethics Committee. Healthy volunteer donor blood (National Health Service Blood and Transplant; Addenbrooke's Hospital, Cambridge University Hospital, UK) was used for the preparation of peripheral blood mononuclear cells (PBMCs) using methodology previously described (Layhadi, Turner, Crossman, & Fountain, 2018). In brief, blood was layered on top of Histopaque-1077 (Sigma Aldrich, Haverhill, UK) for centrifugation at 1,000× *g* for 25 min. Buffy coat layers were collected, and PBMCs were counted. $CD14^+$ monocytes were positively selected from PBMC using anti-$CD14^+$ magnetic beads (Miltenyi Biotech). Monocytes were resuspended in salt buffered solution (SBS) buffer (mM): NaCl, 130; KCl, 5; $MgCl_2$, 1.2; $CaCl_2$, 1.5; D-glucose, 8; HEPES, 10; pH 7.4.

2.2 | Culture of THP-1 human monocyte cells

THP-1 monocyte cells (CLS Cat# 300356/p804_THP-1, RRID: CVCL_0006) were cultured at 37°C, 5% CO_2 in RPMI 1640 medium containing 2-mM L-glutamine and supplemented with 10% (v/v) FBS, 50-IU·ml^{-1} penicillin, and 50-µg·ml^{-1} streptomycin. Cells densities were maintained between 1×10^5 and 1×10^6 cells·ml^{-1}.

2.3 | Intracellular Ca^{2+} measurements

Experiments were conducted as described previously (Micklewright, Layhadi, & Fountain, 2018). Briefly, cells were treated with antagonists or vehicle controls for 30 min prior to challenge with agonists. Measurements were made using a 96-well plate reader with rapid well injection (Flexstation III, Molecular Devices). All experiments were performed in SBS (pH 7.4), containing 130-mM sodium chloride, 5-mM potassium chloride, 1.2-mM magnesium chloride, 1.5-mM calcium chloride, 8-mM D-(+)-glucose, and 10-mM HEPES. The cells were then loaded with 2-µM Fura-2AM (TEF Labs, Austin, TX, USA) in SBS supplemented with 0.01% (w/v) pluronic for 1 hr at 37°C while being protected from light. The loading buffer was then removed, and the cells were washed twice with SBS. Where applicable, the cells were incubated for a further 30 min with antagonists/vehicle or calcium-free SBS (SBS lacking 1.5-mM calcium chloride but containing 2-mM EGTA, pH 7.4). All antagonists were dissolved in water or DMSO. Changes in intracellular Ca^{2+} concentration were measured as the ratio of emission at 510 nm following excitation at 340 and 380 nm (*F ratio*). Cells were treated with antagonists or vehicle controls for 30 min prior to challenge with agonists.

2.4 | Flow cytometry

All sets were conducted at room temperature; 1×10^6 cells·ml^{-1} were prepared in 100-µl PBS for each marker and control experiment. Cells were treated for 30 min with drugs and vehicle controls prior to being labeled with an antibody. Cells were incubated with 5-µg·ml^{-1} human

BD Fc block (BD Pharmingen, New Jersey, USA) for 10 min. Next, (1:100) mouse monoclonal anti-CCR2 PE-conjugated antibody (BioLegend Cat# 357205, RRID:AB_2562058) or isotype control (BioLegend, USA) was added, and cells were incubated in the dark for 30 min. Labelled cells were analysed using a CytoFLEX flow cytometer (Beckman Coulter). Fluorescence intensity was read for PE using 496-nm excitation and 578-nm emission wavelengths, respectively. Living cells were gated according to their forward and side scatter profiles, and then histograms were plotted to compare fluorescence intensity for anti-CCR2 and isotype control antibodies using CytExpert Software (version 1.2.11, Beckman Coulter).

2.5 | siRNA-mediated gene knock-down

THP-1 cells (2×10^5 final) were incubated overnight in complete RPMI (10% FBS) without antibiotics before cells were transfected using Dharmacon siRNA (25-nM final concentration) with DharmaFECT 2 transfection reagent (Dharmacon Research Inc, Cambridge, UK) using the manufacturer's protocol for a 96-well format. Scrambled siRNA and siRNA targeted against GAPDH were used in negative and positive control experiments, respectively.

2.6 | RNA extraction and nonquantitative RT-PCR

Total RNA was extracted from cells using Tri Reagent (Sigma Aldrich) with subsequent DNase I treatment (Ambion). cDNA was synthesised from 1-μg total RNA using Superscript II reverse transcriptase (Invitrogen, Waltham, USA). PCR was performed using a Taq polymerase readymix (Sigma Aldrich) using the primers as given in Table 1.

2.7 | Immunocytochemistry

THP-1 cells were seeded onto poly L-lysine coated coverslips followed by fixation with 4% (w/v) paraformaldehyde for 15 min at room temperature and permeabilisation with 0.25% (v/v) Triton X-100 for 10 min. Fixed and permeabilised cells were blocked with 1% (w/v) BSA. Cells were incubated with primary antibodies overnight at 4°C, followed by washing and incubation with Alexa Fluor 488-conjugated secondary antibodies. In negative control experiments, primary antibodies were omitted. Rabbit polyclonal primary antibodies (anti-DGKδ, Sigma HPA049101, RRID:AB_2680630; anti-DGKγ, Abcam ab151967, RRID:AB_151967; anti-DGKη, Abcam ab80693, RRID:AB_1658681; anti-DGKζ, Abcam ab111047, RRID:AB_10858121; anti-**DAGLα**, Abcam ab106979, RRID:AB_10862875; and anti-**DAGLβ**) were used in conjunction with a goat anti-rabbit secondary antibody (Thermo Fisher Scientific Cat# A27034, RRID:AB_2536097). Mouse monoclonal primary antibodies (anti-**PKCα**, Santa Cruz Biotechnology sc-8393, RRID:AB_628142; anti-DGKα, Santa Cruz Biotechnology sc-271644, RRID:AB_10708574; anti-DGKε, Santa Cruz Biotechnology Cat# sc-100372, RRID:AB_2245858; and anti-DGKθ, Santa Cruz Biotechnology sc-137197, RRID:AB_2292802) were used in conjunction with goat anti-mouse secondary antibody (Thermo Fisher Scientific Cat# A28175, RRID:AB_2536161). Fluorescent and brightfield images were captured using a Zeiss AxioPlan 2ie epifluorescent microscope. The Immuno-related procedures used comply with the recommendations made by the *British Journal of Pharmacology*.

2.8 | Transmigration assays

Transwell migration assays were performed as previously described (Micklewright et al., 2018). Briefly, assays were performed in 24-well plates using polyethylene terephthalate membrane inserts with 3-μm pores; 1×10^6 cells in RPMI (no serum), with vehicle or drug treatment added to the lower chamber. Assays were performed for 2 hr at 37°C, and the cells that had migrated were on the underside of the transwell insert membrane and were stained using crystal violet. The chemotactic index was calculated as the ratio of cells that migrated towards CCL2 over vehicle control. These experiments were blinded.

2.9 | DAG assay

DAG levels were measured using an enzyme-linked fluorescence assay (Cell Biolabs). Accumulation of fluorescence product was measured using 530-nm excitation and 590-nm emission; 5×10^7 THP-1 cells in suspension were incubated at 20°C in SBS solution for 2 hr prior to CCL2 challenge. Cells were exposed to inhibitors for 30 min before challenge with CCL2 or vehicle. Following cell exposure to CCL2 for 1 or 2 min, cells were plunged on ice and sonicated in methanol, followed by extraction of organic phase in chloroform. Total protein was measured by the Bradford assay and used to normalise fluorescence measurements.

2.10 | Cell toxicity assay

Potential cytotoxic effects of drug treatments were measured by quantification of LDH release from cells using a colorimetric assay (Abcam) as described by Campwala et al. (2014). To mimic experimental conditions, 1×10^6 THP-1 or freshly isolated monocytes were incubated with test compounds in SBS assay buffer for 30 min prior to conducting the LDH assay; 0.1% Triton X-100 was used in positive control experiments. These experiments were blinded.

2.11 | Data and statistical analysis

The data and statistical analysis comply with the recommendations on experimental design and analysis in pharmacology (Curtis et al., 2018). Data analysis was performed using Origin Pro 9.0 software (Origin Lab, USA). Dose–response curves were fitted assuming an n_H of 1, with the Hill equation used to determine the degree of cooperation. Figure data points represent mean values ± SEM (error bars); *n* is defined as number of technical repeats or biological repeats (donor number) for experiments with THP-1 cells and freshly isolated $CD14^+$ monocytes, respectively. Statistical significance was

TABLE 1 Expression of DAG kinase, DAG lipase, and PKC mRNA transcripts in $CD14^+$ monocytes and THP-1 cells

Gene	Name	$CD14^+$ monocytes	THP-1 cells
DGKA	DAG kinase α	Expressed	Expressed
Sense	CAACAGGAGGCAAAACTGGC		
Anti-sense	TGCCACCTAGAGATCCACGA		
DGKB	DAG kinase β	Not expressed	Not expressed
Sense	TCTGTGTGCAATGGAGGCAT		
Anti-sense	CCACCCACAACAATCTGTCCA		
DGKD	DAG kinase δ	Expressed	Expressed
Sense	TTATTGGTTGCACGCACAGC		
Anti-sense	CAGACCATCATCAAAGAGGGGA		
DGKE	DAG kinase ε	Expressed	Expressed
Sense	AGAGGGTAAGTCTCGTCCCC		
Anti-sense	CTCTGGGAACAGGCAACGAT		
DGKG	DAG kinase γ	Expressed	Expressed
Sense	GACTTCTCACCTGGCCTGTC		
Anti-sense	GTCCCTCGGTCTTCAAGCTC		
DGKH	DAG kinase η	Expressed	Expressed
Sense	TATCCCCAGATCCAGGCTGT		
Anti-sense	CAGATGCAGCTATGCTCCCA		
DGKI	DAG kinase ι	Not expressed	Not expressed
Sense	TCCAGTGTGACATGGGCATC		
Anti-sense	GGTACCTGAATCCACGGCAA		
DGKK	DAG kinase κ	Expressed	Not expressed
Sense	CACTGGGCAATGCGATGATG		
Anti-sense	TAACCAGACAAGCCCACGAC		
DGKQ	DAG kinase θ	Expressed	Expressed
Sense	AGGCTCCGAGAGTGACTGAT		
Anti-sense	GTGAACCCCAAGAGTGGAGG		
DGKZ	DAG kinase ζ	Expressed	Expressed
Sense	GGCTCAGGTCGAAGACTTGT		
Anti-sense	CAGGATGCTGCAGAAGTCAGT		
DAGLA	DAG lipase α	Expressed	Expressed
Sense	TGTCGGATGGCACAATGTCA		
Anti-sense	GAGCCCAGGATGGAGGTGG		
DAGLB	DAG lipase β	Expressed	Expressed
Sense	GTTCGTACCACAAACCGTGC		
Anti-sense	CTCCCAGGAAGCTGATCTGGA		
PRKCA	PKCα	Expressed	Expressed
Sense	CCTTTGCCACACACTTTGGG		
Anti-sense	TGACCGAGTGAAACTCACGG		
PRKCB	PKCβ	Expressed	Expressed
Sense	TCTCTTGTCTCTAGCTTTTGGCT		
Anti-sense	CCCGGAAGAAAAGACGACCA		
PRKCG	PKCγ	Not expressed	Not expressed
Sense	TCTAGAATGGGACAGGGGGT		

(Continues)

TABLE 1 (Continued)

Gene	Name	$CD14^+$ monocytes	THP-1 cells
Anti-sense	CAGGACAGCCTCCCTTCGAT		
PRKCD	PKCδ	Expressed	Expressed
Sense	TGTTGAGGCCCCAGACAAAG		
Anti-sense	TGGTGGTTGGTGCGTTGTAG		
PRKCE	PKCε	Expressed	Expressed
Sense	GGTGCAGACTTGACACTGGT		
Anti-sense	GAACCCGGCGAGGAAATACA		
PRKCH	PKCη	Not expressed	Expressed
Sense	GATCCACCCAACCCTCGAA		
Anti-sense	GCGGGGGTTCTGTGAACTTG		
PRKCQ	PKCθ	Expressed	Expressed
Sense	TTAAGCAGCGAGCCTGTTGA		
Anti-sense	GAAACCTCAAGGCCGAATGC		
PRKCI	PKCι	Expressed	Expressed
Sense	CCCTGGTGTTCATTGCCTCT		
Anti-sense	GGCCTTTGCAATGAGGTTCG		
PRKCZ	PKCζ	Expressed	Expressed
Sense	TGGCTTAAGGTCCTCCGAGT		
Anti-sense	GAGTTCCGCGGAGTTGACC		

Note. Data are representative of five donors/independent experiments. Sense and anti-sense primer sequences used for nonquantitative RT-PCR are given beneath each gene assayed. Positive control PCR products were generated for all primers sets using human brain cDNA template.

determined using Student's paired *t* test for two samples and ANOVA for multiple sample datasets. A confidence interval of 5% ($P < .05$) is applied throughout.

2.12 | Blinding in experiments

Experimental manipulations were blinded to the experimenter where technically feasible.

2.13 | Chemicals and reagents

Unless otherwise stated, all chemicals and reagents were purchased from Sigma Aldrich.

2.14 | Nomenclature of targets and ligands

Key protein targets in this article are hyperlinked to corresponding entries in http://www.guidetopharmacology.org, the common portal for data from IUPHAR/BPS Guide to PHARMACOLOGY (Harding et al., 2018), and are permanently archived in the Concise Guide to PHARMACOLOGY 2017/2018 (Alexander, Christopoulos et al., 2017; Alexander, Fabbro et al., 2017).

3 | RESULTS

3.1 | DAG kinase and DAG lipase inhibitors attenuate CCL2-evoked intracellular Ca^{2+} signals and migration in freshly isolated human monocytes and THP-1 monocytic cells

CCL2 evoked concentration-dependent intracellular Ca^{2+} responses in freshly isolated human $CD14^+$ monocytes (Figure 1a) with an EC_{50} of 33 ± 4 nM (n = 8; Figure 1b). These responses were abolished by the CCR2 selective antagonist BMSCCR222 (Figure 1c; IC_{50} 9.2 ± 1.2 nM, n = 8). CCL2 also evoked Ca^{2+} responses in THP-1 monocytes (Figure 1d) with an EC_{50} 45 ± 12 nM (n = 6; Figure 1e), and these responses were abolished by BMSCCR222 (Figure 1f; IC_{50} 8.4 ± 1.4 nM, n = 6). These data demonstrate that CCL2-evoked intracellular Ca^{2+} responses are dependent upon CCR2 activation in both freshly isolated monocytes and the THP-1 monocytic cells. CCL2-evoked intracellular Ca^{2+} responses in freshly isolated monocytes (Figure 1a) and THP-1 monocytic cells (Figure 1d) were abolished following PLC inhibition with **U73122**.

CCR2 is a G_i-coupled GPCR that elicits intracellular Ca^{2+} responses in a pertussis toxin-sensitive and PLC-dependent fashion (Campwala et al., 2014). This signal transduction mechanism generates DAG, and we therefore investigated the impact of DAG metabolism on CCL2-evoked Ca^{2+} responses. In THP-1 monocytes, **R59949** (a small molecule inhibitor of DAG kinase; de Chaffoy de Courcelles et al.,

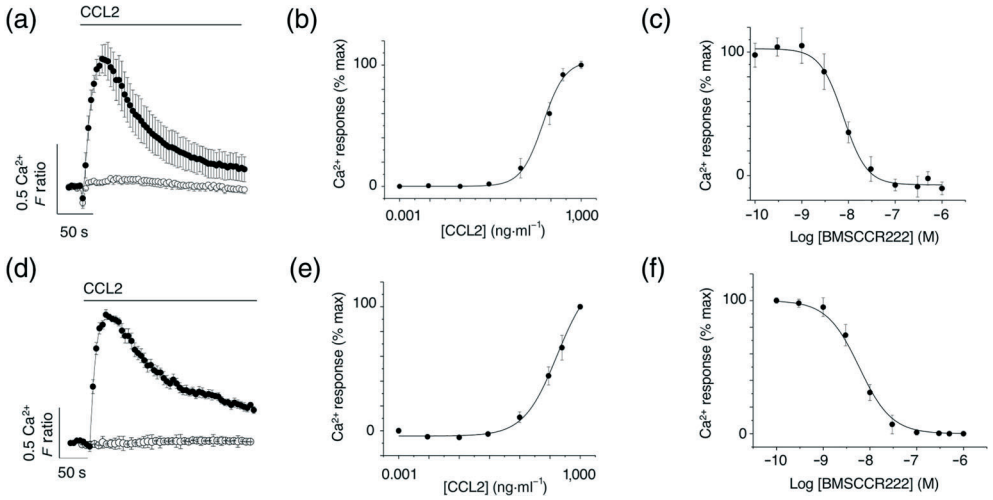

FIGURE 1 CCR2 is the cognate receptor for CCL2 in freshly isolated human monocytes and THP-1 monocytic cells. (a) Averaged (n = 8) intracellular Ca^{2+} response to CCL2 (50 ng·ml^{-1}) in freshly isolated CD14^{+} human monocytes. Response in the presence (open circles) and absence (closed circles) of 5-μM U73122 (n = 6; P < .05). (b) Concentration–response curve for CCL2-evoked responses in freshly isolated monocytes (n = 8; EC_{50} = 33 ± 4 nM). (c) Concentration–inhibition curve for selective CCR2 antagonist BMSCCR222 (IC_{50} = 9 ± 1 nM; n = 8) against Ca^{2+} responses evoked by CCL2 (50 ng·ml^{-1}) in freshly isolated monocytes. (d) Averaged (n = 6) intracellular Ca^{2+} response to CCL2 (50 ng·ml^{-1}) in THP-1 cells. Response in the presence (open circles) and absence (closed circles) of 5-μM U73122 (n = 6; P < .05). (e) Concentration–response curve for CCL2-evoked responses in THP-1 cells (n = 6; EC_{50} = 45 ± 12 nM). (f) Concentration–inhibition curve for BMSCCR222 (IC_{50} = 8 ± 1 nM; n = 6) against Ca^{2+} responses evoked by CCL2 (50 ng·ml^{-1}) in THP-1 cells. F ratio is the Ca^{2+} response as measured by the Fura-2 emission intensity ratio when excited at 340 and 380 nm. Data in concentration–response/inhibition curves are expressed as a percentage of the control response in the presence of vehicle alone

1989) attenuated CCL2-evoked Ca^{2+} signalling (Figure 2a) with a half-maximal concentration of 8.6 ± 1.2 μM (n = 7; Figure 2b). Maximal response in THP-1 cells was inhibited by approximately 70% using 30-μM R59949 (Figure 2c). Similarly, CCL2-evoked Ca^{2+} responses were suppressed by **RHC80267** (Figure 2d), an inhibitor of DAG lipase (Dale & Penfield, 1987). RHC80267 inhibited the response with a half-maximal concentration of 9.3 ± 1.0 μM (n = 7; Figure 2e), reducing the maximal response to CCL2 by approximately 30% using 30-μM RHC80267 (Figure 2f). In addition to CCL2-evoked Ca^{2+} signals, inhibition of both DAG kinase and DAG lipase attenuated CCL2-mediated THP-1 chemotaxis (Figure 2g). Application of CCL2 to THP-1 monocytic cells caused a rapid increase in cellular DAG (Figure 2h). As for CCL2-evoked Ca^{2+} signals (Figure 1d), PLC inhibition with U73122 attenuated the CCL-2 evoked increase in cellular DAG (Figure 2h). Both R59949 and RHC80267 significantly enhanced CCL2-evoked DAG elevation (Figure 2h), consistent with a role of DAG kinase and DAG lipase in metabolising DAG following receptor-mediated synthesis.

Importantly, inhibiting DAG kinase and DAG lipase attenuated CCL2-evoked signalling in freshly isolated human CD14^{+} monocytes (Figure 3). R59949 (30 μM; Figure 3a) and RHC80267 (30 μM; Figure 3b) inhibited CCL2-evoked Ca^{2+} signals, inhibiting the peak Ca^{2+} response by approximately 75% and 30% (Figure 3c), respectively. Furthermore, inhibiting both DAG kinase and DAG lipase attenated CCL2-stimulated migration in freshly isolated monocytes (Figure 3d). Interestingly, intracellular Ca^{2+} responses elicited as a consequence of activation of the **formyl peptide receptor** on monocytes with **n-formylmethionine-leucyl-phenylalanine (fMLP)** was insensitive to either R59949 (Figure 3e) or RHC80267 (Figure 3f), which suggests that neither DAG kinase nor DAG lipase inhibition is a generic regulator of receptor-mediated Ca^{2+} signalling in monocytes (Figure 3g). Although the focus of this study is CCL2, we also investigated the effect of R59949 and RHC80267 on **CCL5**-mediated responses in freshly isolated monocytes. CCL5 has been reported to activate the chemokine receptors **CCR1**, **CCR3**, and **CCR5** (de Wit, de Munnik, Leurs, Wischer, & Smit, 2016) and is also implicated in the onset and progression of atherosclerosis (Schober et al., 2002). In monocytes, we observed that CCL5 mediates intracellular Ca^{2+} response through activation of CCR1, but not CCR3 or CCR5 (Figure S1). The activity of CCR1 is also attenuated following DAG kinase or DAG lipase inhibition. However, the ability of **CXCL1**, which is implicated in monocyte mobilisation under chronic inflammatory conditions (Drechsler, Duchene, & Soehnlein, 2015), to evoke intracellular Ca^{2+} responses in monocytes was attenuated by inhibition of DAG kinase but not DAG lipase (Figure S2). In monocytes, we observed that CXCL1-evoked Ca^{2+} responses are mediated by **CXCR2** activation (Figure S2).

Next, we profiled the expression of DAG kinase and DAG lipase isoforms expressed in freshly isolated human CD14^{+} monocytes and THP-1 monocytic cells. RT-PCR analysis of mRNA transcripts revealed an overlapping expression profile of DAG kinase and DAG lipase isoforms in CD14^{+} monocytes and THP-1 cells (Table 1). For DAG kinase isoforms, α, γ, δ, η, ε, θ, κ, and ζ were expressed by both cell types, and β and ι were not. For DAG lipase isoforms, isoforms α and β were expressed by CD14^{+} monocytes and THP-1 cells (Table 1). To corroborate these findings, we confirmed expression at the protein level by immunocytochemistry in THP-1 cells (Figure S3).

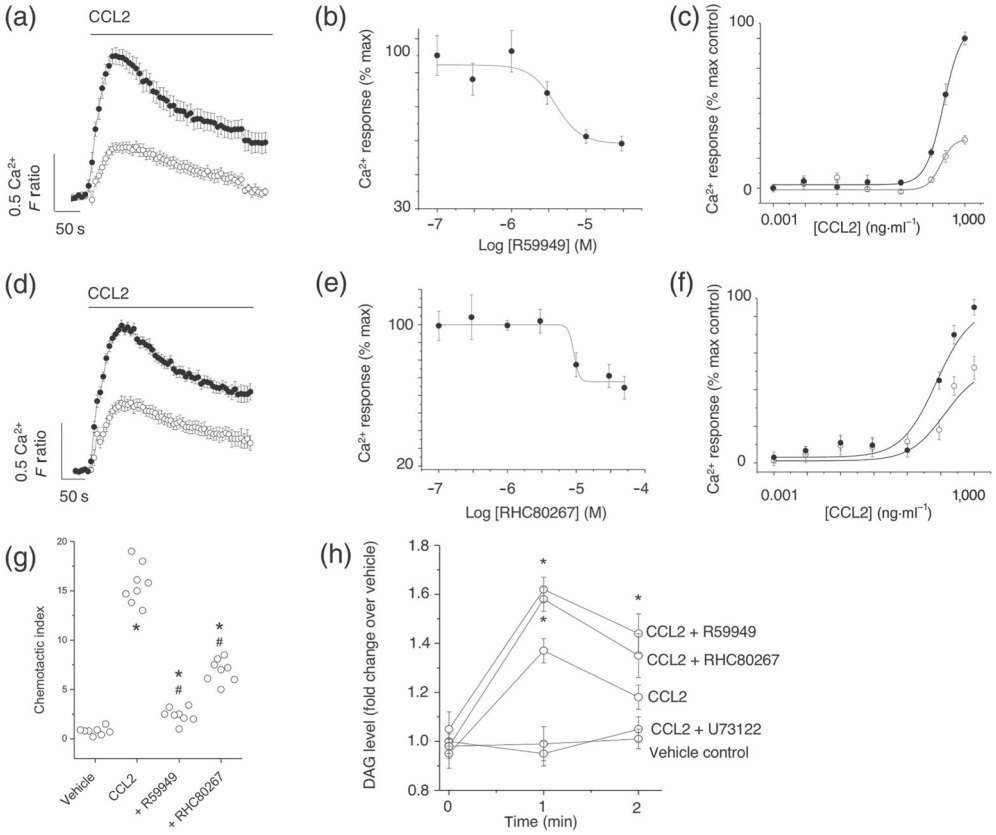

FIGURE 2 Inhibitors of DAG kinase and DAG lipase attenuate CCL2-evoked Ca^{2+} signalling and migration in THP-1 cells. (a) Effect of DAG kinase inhibitor R59949 (30 μM) on Ca^{2+} responses evoked by CCL2 (50 ng·ml^{-1}; n = 7). Averaged responses are shown in the presence of vehicle (closed circles) and inhibitor (open circles). (b) R59949 concentration–inhibition curve (IC_{50} = 9 ± 1 μM; n = 7) against Ca^{2+} responses evoked by CCL2 (50 ng·ml^{-1}). (c) Effect of 30-μM R59949 on CCL2 concentration–response curve (n = 7). (d) Effect of DAG lipase inhibitor RHC80267 (30 μM) on Ca^{2+} responses evoked by CCL2 (50 ng·ml^{-1}; n = 7). Averaged responses are shown in the presence of vehicle (closed circles) and inhibitor (open circles). (e) RHC80267 concentration–inhibition curve (IC_{50} = 9 ± 1 μM; n = 7) against Ca^{2+} responses evoked by CCL2 (50 ng·ml^{-1}). (f) Effect of 30-μM RHC80267 on CCL2 concentration–response curve (n = 7). (g) Effect of R59949 (30 μM) and RHC80267 (30 μM) on THP-1 transmigration to CCL2 (3 ng·ml^{-1}). *P < .05 versus vehicle and $^{\#}P$ < .05 versus CCL2 alone (n = 8). F ratio is the Ca^{2+} response as measured by the Fura-2 emission intensity ratio when excited at 340 and 380 nm. Data in concentration–response/inhibition curves are expressed as a percentage of the control response in the presence of vehicle alone. (h) Biochemical measurement of DAG changes in THP-1 cells. Cells preincubated for 30 min with U73122 (5 μM), R59949 (30 μM), or RHC80267 (30 μM) prior to CCL2 challenge (50 ng·ml^{-1}) for 1 or 2 min (n = 6). Vehicle control; cells are preincubated with vehicle and not challenged with CCL2. *P < .05 versus CCL2 alone

3.2 | The amount of cell surface CCR2 is unaffected by DAG kinase or DAG lipase inhibition

A possible mechanism underlying the reduced responsivity to CCL2 following inhibition of DAG metabolism is a reduction in the number of cell surface CCR2 receptors. To test this hypothesis, we quantified CCR2 cell surface expression in freshly isolated monocytes and THP-1 cells following R59949 or RHC80267 treatment by flow cytometry. A PE-conjugated antibody recognising human CCR2 labelled CCR2 CD14^{+} monocytes (Figure 4a) and THP-1 cells (Figure 4b) over an isotype control. R59949 and RHC80267 were applied to cells to mimic the protocol used to investigating Ca^{2+} signalling. Despite this, neither R59949 nor RHC80267 had any significant effect on CCR2 cell surface expression in THP-1 cells or human CD14^{+} monocytes (Figure 4).

To further understand the role of DAG kinase and DAG lipase activity in shaping CCL2-evoked intracellular Ca^{2+} responses, we examined the effect of the inhibitors on the responses in the absence of extracellular Ca^{2+} to negate Ca^{2+} entry. Under these conditions, CCL2 evoked a rapidly rising but transient Ca^{2+} response which returned to baseline (Figure 5a). DAG kinase inhibition with R5549 attenuated the peak response but lead to a sustained plateau phase after the transient response (Figure 5a,b), exemplified by an increased AUC (Figure 5c). Unlike DAG kinase inhibition, DAG lipase inhibition with RHC80267 did not affect the transient phase (Figure 5d,e) but did lead to a sustained plateau phase after the transient response (Figure 5f). The AUC for CCL2-evoked responses under conditions of no external Ca^{2+} was significantly large following DAG lipase inhibition compared to DAG kinase inhibition, reflecting the difference in degree of inhibition observed in conditions with external Ca^{2+} (Figure 2). These data suggest that although both DAG kinase inhibition and DAG lipase inhibition suppress the global Ca^{2+} response to CCL2, they may do so via different mechanisms.

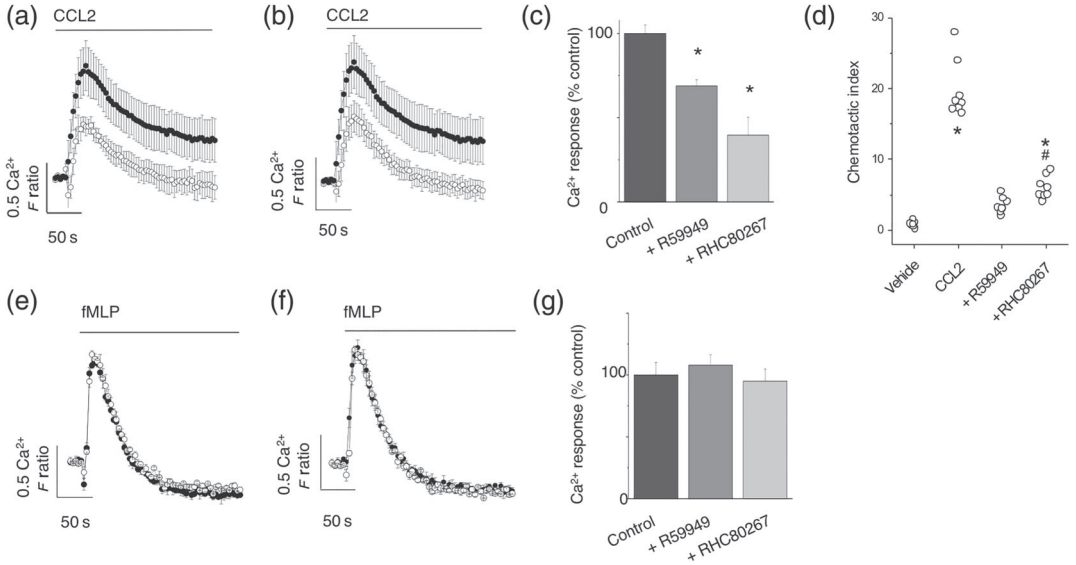

FIGURE 3 Responses to CCL2 but not fMLP are attenuated by DAG kinase and DAG lipase inhibitors in freshly isolated human monocytes. Effect of (a) DAG kinase inhibitor R59949 (30 μM) and (b) DAG lipase inhibitor RHC80267 (30 μM) on Ca^{2+} responses evoked by CCL2 (50 ng·ml^{-1}) in monocytes (n = 8). Averaged responses are shown in the presence of vehicle (closed circles) and inhibitor (open circles). (c) Bar chart showing effect of R59949 (30 μM) and RHC80267 (30 μM) on the peak Ca^{2+} response evoked by CCL2 (50 ng·ml^{-1}; n = 8). (d) Effect of R59949 (30 μM) and RHC80267 (30 μM) on freshly isolated monocyte transmigration to CCL2 (3 ng·ml^{-1}). $^{*}P$ < .05 versus vehicle and $^{\#}P$ < .05 versus CCL2 alone (n = 8). Lack of effect of (e) R59949 (30 μM) or (f) RHC80267 (30 μM) on Ca^{2+} responses evoked by fMLP (10 μM) in monocytes (n = 6). Averaged responses are shown in the presence of vehicle (closed circles) and inhibitor (open circles). (g) Bar chart showing lack of effect of R59949 (30 μM) and RHC80267 (30 μM) on peak Ca^{2+} response evoked by fMLP (10 μM; n = 6). F ratio is the Ca^{2+} response as measured by the Fura-2 emission intensity ratio when excited at 340 and 380 nm. Data in inhibition experiments are expressed as a percentage of the control response in the presence of vehicle alone

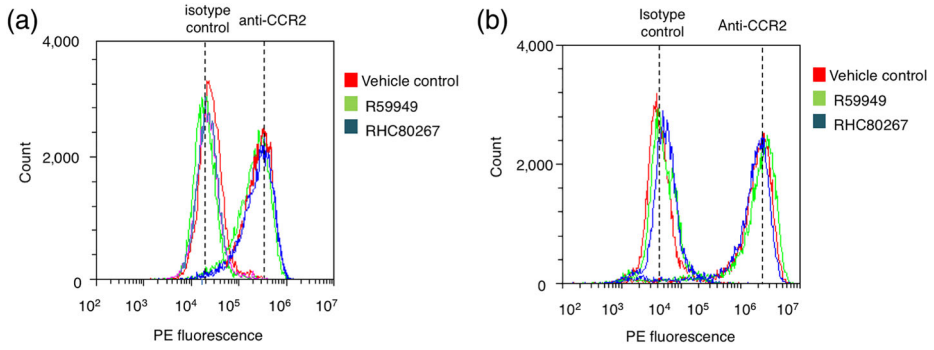

FIGURE 4 Inhibition of DAG kinase or DAG lipase does not reduce the cell surface population of CCR2 in freshly isolated monocytes and THP-1 cells. Three representative (n = 6) flow cytometry profiles of freshly isolated CD14^{+} monocytes (a) and THP-1 cells (b) labelled with anti-CCR2 antibodies or isotype control. Cells were treated with vehicle control, R59949 (30 μM), or RHC80267 (30 μM). Anti-CCR2 cell surface immunoreactivity is indistinguishable between vehicle control and test groups

3.3 | Attenuating effect of DAG metabolism inhibitors is mimicked by 1-oleoyl-2-acetyl-sn-glycerol but not rescued by phosphatidylinositol 4,5-bisphosphate

Following receptor-mediated hydrolysis of **PIP_2** to DAG and **IP_3**, DAG is used as a substrate for the rapid resynthesis of PIP_2. We therefore reasoned that limiting DAG metabolism could therefore limit PIP_2 resynthesis and reduce the pool of PIP_2 available for receptor-mediated hydrolysis, this in time could underlie the attenuated CCL2-mediated Ca^{2+} response observed. To this end, we attempted to reverse the effect of DAG kinase inhibition by supplementing cells with exogenous PIP_2 (Kantonen et al., 2011). However, in these experiments, exogenous PIP_2 did not limit the ability of R59949 to suppress CCL2-evoked Ca^{2+} signals (Figures 6a,b), suggesting that PIP_2 availability did not underlie the inhibition. We therefore attempted to address whether the accumulation of DAG itself following pharmacological inhibition of its metabolism could mediate the attenuation of Ca^{2+} signalling. We observed that **1-oleoyl-2-acetyl-sn-glycerol (OAG)**, a membrane permeable DAG analogue (Assani et al., 2017), could mimic the effect of DAG kinase inhibition or DAG lipase inhibition (Figure 6c) and inhibit CCL2-evoked Ca^{2+} signalling in a

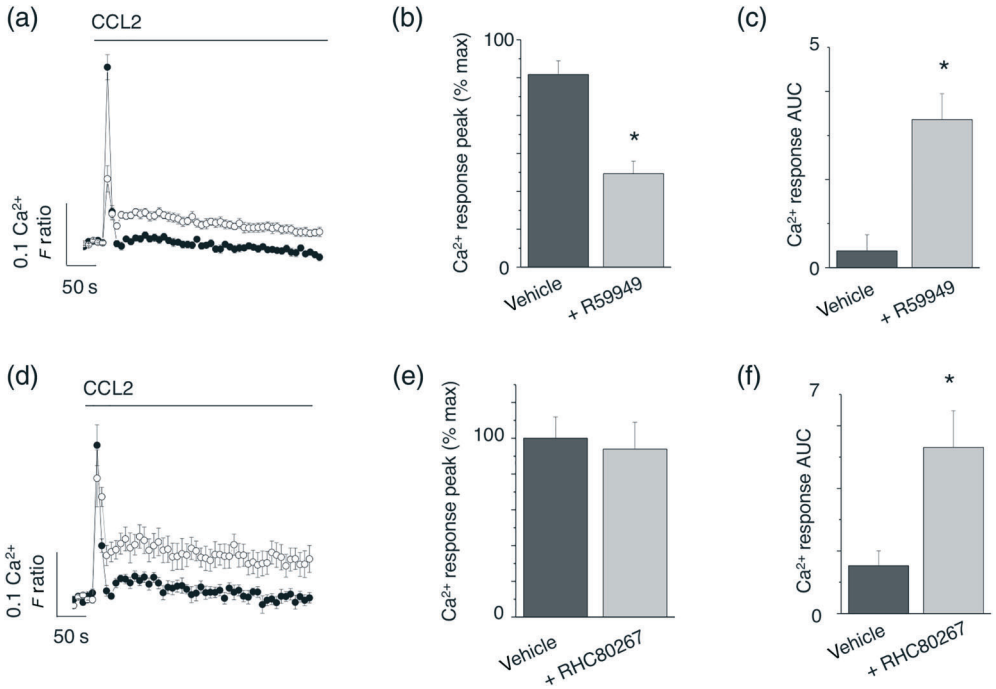

FIGURE 5 Effects of DAG kinase and DAG lipase inhibitors on CCL2-evoked Ca^{2+} responses in THP-1 cells in the absence of extracellular Ca^{2+}. (a) Averaged (n = 8) intracellular Ca^{2+} responses evoked by CCL2 (50 ng·ml^{-1}) in the absence of extracellular Ca^{2+} and presence (open circles) and absence (closed circles) of R59949 (30 μM). (b) and (c) show the effect of R59949 on intracellular Ca^{2+} peak and AUC in the absence of extracellular Ca^{2+} (n = 8). (d) Averaged (n = 8) intracellular Ca^{2+} responses evoked by CCL2 (50 ng·ml^{-1}) in the absence of extracellular Ca^{2+} and presence (open circles) and absence (closed circles) of RHC80267 (30 μM). (e) and (f) show the effect of R59949 on intracellular Ca^{2+} peak and AUC in the absence of extracellular Ca^{2+} (n = 8). *P < .05 versus vehicle control for all

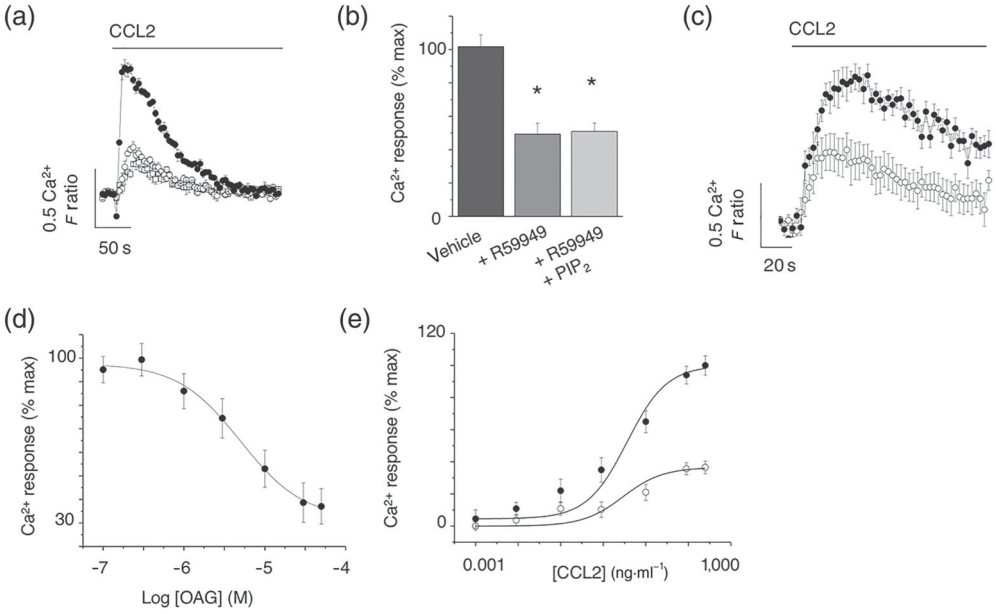

FIGURE 6 Application of exogenous PIP_2 does not rescue CCL2-evoked Ca^{2+} response following DAG kinase inhibition, but inhibition is mimicked by OAG in THP-1 cells. (a) CCL2-evoked (50 ng·ml^{-1}) intracellular Ca^{2+} responses in the presence of vehicle control (closed circles), R59949 (open circles; 30 μM), or R59949 plus exogenous PIP_2 (squares; 300 μM; n = 8). (b) Bar chart showing average peak intracellular Ca^{2+} responses. *P < .05 versus vehicle control. (c) CCL2-evoked (50 ng·ml^{-1}) intracellular Ca^{2+} responses in the presence of vehicle control (closed circles) or cell permeable DAG analogue, OAG (open circles; n = 8). (d) Concentration–inhibition curve for OAG effect on intracellular Ca^{2+} responses evoked by CCL2 (50 ng·ml^{-1}; n = 8). (e) Effect of OAG (30 μM) on CCL2 concentration–response curve in THP-1 cells (IC_{50} 9 ± 1 μM; n = 6). Responses are in the presence of vehicle control (closed circles) or OAG (open circles). F ratio is the Ca^{2+} response as measured by the Fura-2 emission intensity ratio when excited at 340 and 380 nm. Data in inhibition experiments are expressed as a percentage of the control response in the presence of vehicle alone

concentration fashion (Figure 6d). The half-maximal concentration for OAG was 9.2 ± 1.2 μM (n = 6), and the maximum CCL2 response was suppressed by approximately 70% at 30-μM OAG (Figure 6e).

3.4 | Differential dependency on PKC for effects of DAG metabolism inhibitors and OAG

As DAG is a well-characterised activator of **PKC**, we sought to test whether PKC activity was required for the suppressive action of OAG, DAG kinase inhibition, and DAG lipase inhibition. RT-PCR analysis of PKC isoform mRNA transcripts revealed expression of α, β, δ, η, ε, θ, ι, and ζ but not γ in THP-1 cells (Table 1). We confirmed the expression of PKCα by immunocytochemistry (Figure S3). The expression pattern was the same in freshly isolated $CD14^+$ monocytes except that PKCε was not expressed (Table 1). Due to the diverse repertoire of PKC isoforms expressed, we employed pharmacological tools that allowed discrimination between classical DAG and Ca^{2+}-dependent isoforms (α, β, and γ; blocked by **Gö6976**) and DAG dependent but Ca^{2+}-independent isoforms (δ, ε, η, or θ; blocked by **Gö6983**); Gö6983 also blocks α, β, and γ isoforms (Goekjian & Jirousek, 1999; Gschwendt et al., 1996). Gö6983 100-nM (Young, Rey, Sinnett-Smith, & Rozengurt, 2014) had no effect on the control Ca^{2+} response to CCL2 (Figure 7a); however, 100-nM Gö6976 (Lin, Leu, Huang, & Tsai, 2011) significantly inhibited the response (Figure 7a). Gö6983 could rescue the response inhibited by OAG (Figure 7b), R59949 (Figure 7c), or RHC80267 (Figure 7d), though Gö6976 could not (Figure 7b–d). These data, summarised in Figure 7 e, suggest that the inhibitory action of exogenous DAG (OAG) on DAG metabolism is mediated via a Ca^{2+}-independent PKC isoform. The inhibitory action of R59949 and RHC80267 on CCL2-evoked Ca^{2+} in freshly isolated monocytes could also be reversed by Gö6983 (n = 5; Figure 7f).

3.5 | The Ca^{2+}-sensitive isoform PKCα regulates CCL2-evoked Ca^{2+} signalling in THP-1 cells

A striking observation of the experiments with Gö6976 was its ability to inhibit CCL2-evoked Ca^{2+} signalling without pharmacological manipulation of DAG metabolism. These data suggest that a DAG and Ca^{2+}-dependent PKC isoform may regulate the CCL2 response, and to investigate this further, we attempted siRNA-mediated knock-down studies of the classical Ca^{2+}-sensitive PKC isoform PKCα. In these experiments, siRNA delivery to THP-1 monocytes could inhibit CCL2-evoked Ca^{2+} responses versus scrambled siRNA counterparts (Figure 8a). Though the response peak was unaffected (Figure 8b), PKCα knock-down significantly reduced response AUC (Figure 8c). Quantitative RT-PCR confirmed PKCα mRNA knock-down

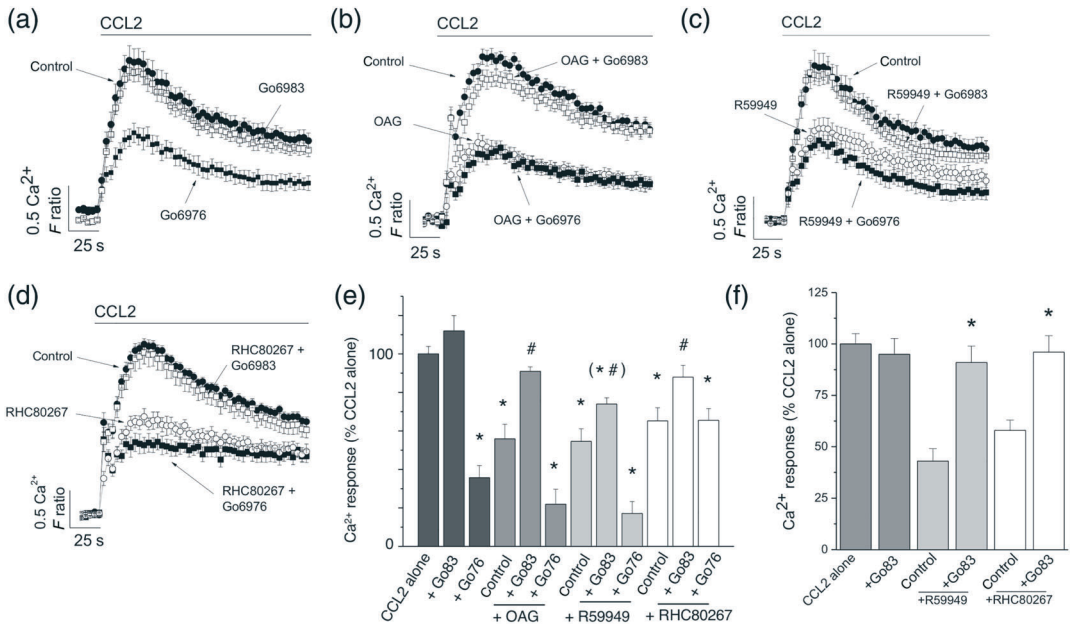

FIGURE 7 Effect of inhibiting Ca^{2+}-dependent and Ca^{2+}-independent PKC isoforms on CCL2-evoked responses following inhibition of DAG kinase and DAG lipase in THP-1 cells and freshly isolated monocytes. (a) CCL2-evoked intracellular Ca^{2+} responses in THP-1 cells in the presence of vehicle control, Gö6976 (100 nM), or Gö6983 (100 nM; n = 8). (b) CCL2-evoked intracellular Ca^{2+} responses in THP-1 cells in the presence of vehicle control and OAG (30 μM) in the presence and absence of Gö6976 or Gö6983 (n = 8). (c) CCL2-evoked intracellular Ca^{2+} responses in THP-1 cells in the presence of vehicle control and R59949 (30 μM) in the presence and absence of Gö6976 or Gö6983 (n = 8). (d) CCL2-evoked intracellular Ca^{2+} responses in THP-1 cells in the presence of vehicle control and RHC80267 (30 μM) in the presence and absence of Gö6976 or Gö6983 (n = 8). (e) Bar chart showing averaged data from experiments (a–d). (f) Bar chart showing CCL2-evoked Ca^{2+} responses in freshly isolated monocytes and the effect of R59949 (30 μM) and RHC80267 (30 μM), in the presence and absence of Gö6983 (100 nM; n = 8). All intracellular Ca^{2+} responses were evoked by 50-ng·ml^{-1} CCL2. $^*P < .05$ versus CCL2 and $^{\#}P < .05$ for combined inhibitors compared to OAG, R59949, or RHC80267 alone. F ratio is the Ca^{2+} response as measured by the Fura-2 emission intensity ratio when excited at 340 and 380 nm. Data in inhibition experiments are expressed as a percentage of the control response in the presence of vehicle alone

of approximately 50% versus scrambled siRNA counterparts (Figure 8 d). These data suggest that the activity of PKCα is required for THP-1 cells to respond to CCL2 at control levels.

LDH release assays were performed to test for potential cytotoxic effects of inhibitor treatments applied throughout the study (Figure S4).

4 | DISCUSSION

This study reconfirms that CCR2 is the cognate receptor for CCL2 in human $CD14^+$ monocytes and THP-1 cells. We also provide molecular and function evidence that both DAG kinase and DAG lipase are functional routes for the metabolism of DAG arising from receptor-mediated DAG production. These results corroborate studies in T-lymphocytes (Lee, Kim, Beste, Korestzky, & Hammer, 2012) and cancer cells (Rainero et al., 2014) that demonstrate a role for DAG kinases in modulating chemokine functionality. Our data also reveal that CCL5 signalling via CCR1 is regulated by both DAG kinase activity and DAG lipase activity, though lack of effect of DAG lipase inhibition on CXCL1–CXCR2 signalling is suggestive that this mechanism cannot be generalised for all chemokine action at monocytes.

The data suggest that inhibitors of both DAG kinase and DAG lipase are effective in reducing the efficacy of CCL2 signalling in monocytes, as the response maxima are significantly attenuated with little change in CCL2 EC_{50} values. As the effects of DAG kinase inhibition and DAG lipase inhibition are mimicked by OAG and not rescued by addition of exogenous PIP_2, the effect on CCL2 signalling of inhibiting DAG metabolism is likely to be due to the accumulation of DAG rather than limitation of a DAG metabolite or PIP_2 synthesis. If this is the case, the data suggest that there is no redundancy between kinase- or lipase-dependent metabolic pathways for DAG in human monocytes and processes that modulate the activity of these enzymes have the potential to modulate CCL2 signalling efficacy. Although CCR2 receptors are classical GPCRs and can undergo internalisation as part of mechanisms of receptor desensitisation (Dzenko, Andjelkovic, Kuziel, & Pachter, 2001; Volpe et al., 2012), the data presented here suggest that the mechanism via which inhibition of DAG metabolism causes loss of CCL2 signalling efficacy is not via a reduction in the cell surface population of CCR2 receptors. This therefore suggests that the inhibitory mechanism must involve modulation of the CCR2 receptor itself, an auxiliary subunit or a downstream effector protein. As the effects of OAG, DAG kinase inhibition, and DAG lipase inhibition are reversed by the broadspectrum PKC inhibitor Gö6983 but not Gö6976, a selective inhibitor of Ca^{2+}-dependent PKC isoforms, this suggests that the inhibitor effects of DAG accumulation are mediated by a Ca^{2+}-independent PKC isoform. Analysis of PKC isoform expression suggests that PKCδ, PKCε, PKCη, PKCθ, and PKCζ are potential effectors of the inhibitory actions of DAG in monocytes. Previous studies in

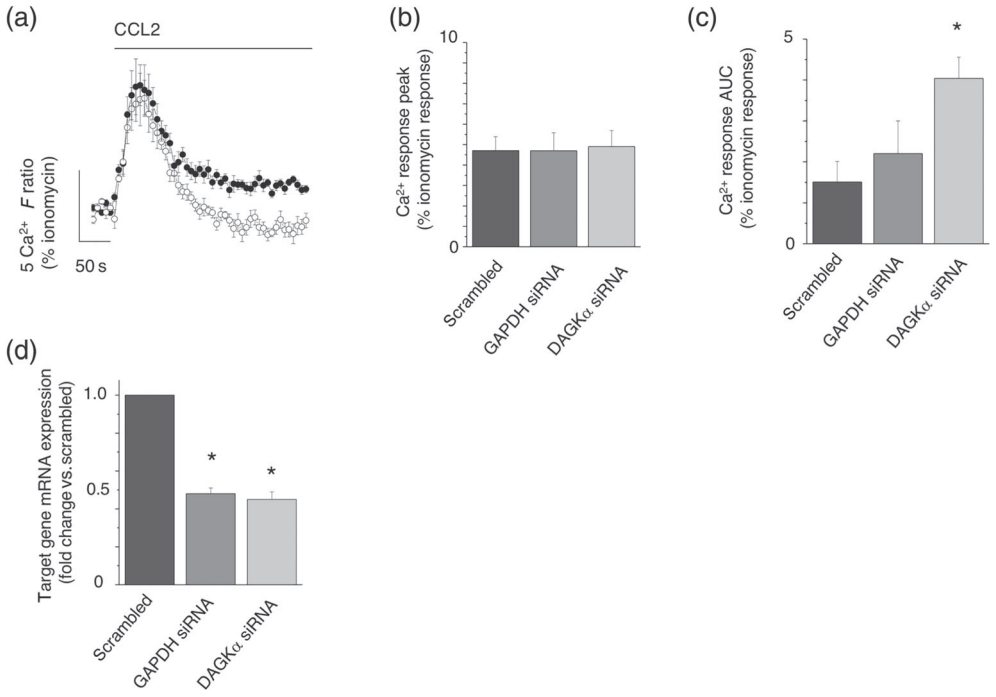

FIGURE 8 Effect of DAG kinase α knock-down of CCL2-evoked Ca^{2+} responses in THP-1 cells. (a) Averaged intracellular Ca^{2+} response evoked by CCL2 in THP-1 cells transfected with scrambled siRNA (closed circles) or DAG kinase α targeted siRNA (open circles; $n = 8$). Bar charts showing peak (b) and AUC (c) intracellular Ca^{2+} responses evoked by CCL2 in scrambled, GAPDH knock-down, or DAG kinase α knock-down THP-1 cells ($n = 8$). (d) qRT-PCR analysis of GAPDH or DAG kinase α mRNA transcripts in scrambled and knock-down THP-1 cells ($n = 8$). *F* ratio is the Ca^{2+} response as measured by the Fura-2 emission intensity ratio when excited at 340 and 380 nm. Responses evoked by 50-ng·ml^{-1} CCL2 for all experiments. *$P < .05$ versus scrambled control cells in all experiments. Data in each experiment are expressed as a percentage of the Ca^{2+} response evoked by ionomycin in control for cell number in knock-down studies

monocytes have documented translocation of both Ca^{2+}-dependent and Ca^{2+}-independent PKC isoforms from the cytoplasm to the plasma membrane upon stimulation with CCL2 (Zhang, Hodge, Rogers, & Oppenheim, 2003). However, opioid receptor activation, which inhibits CCL2 signalling via heterologous desensitisation, causes membrane recruitment of only Ca^{2+}-independent PKC isoforms (Zhang et al., 2003). Such studies support a role for Ca^{2+}-independent PKC isoforms as negative regulators of CCR2 receptor activity. The target of PKC is unlikely to be the CCR2 receptor itself as consensus sequences for PKC-dependent phosphorylation are absent from the cytoplasmic sections of the receptors, although other chemokine receptors, such as CXCR4, are phosphorylated directly by PKC (Luo, Busillo, Stumm, & Benovic, 2017).

The intracellular Ca^{2+} signal generated following CCR2 activation in monocytes most likely involves direct release of Ca^{2+} from ER stores but also Ca^{2+} through plasma membrane channels (Nardelli et al., 1999). Experiments in the absence of extracellular Ca^{2+} support this as CCL2 can still elicit a response though transient and lacking a substantial plateau phase. The shape of the intracellular Ca^{2+} response is also differentially modulated by DAG kinase and DAG lipase inhibitors when the possibility of Ca^{2+} influx is negated. Both R59949 and RHC80267 elevate the plateau phase of release, but only R59949 inhibits the peak Ca^{2+} response in the absence of extracellular Ca^{2+}. This suggests that there may be some discrimination regarding how DAG elevation, directly or indirectly, regulates the ability of CCR2 to release stored Ca^{2+} (Bartlett, Metzger, Gaspers, & Thomas, 2015). Monocytes express a large repertoire of DAG kinase isoforms, and as R59949 is a pan DAG kinase inhibitor, we cannot determine whether redundancy exists between isoforms or whether only some subtypes participate in the regulation of CCR2 activity. siRNA-mediated knock-down studies reveal DAG kinase α as a candidate, at least in THP-1 cells. DAG kinase α has been implicated previously in immune cell function (Sanjuan et al., 2003).

In summary, we demonstrate that inhibition of DAG kinase and DAG lipase is a novel pharmacological route to suppress CCL2-mediated intracellular Ca^{2+} signalling and migration in human monocytes. We suggest that the underlying mechanism involves DAG accumulation and activation of Ca^{2+}-independent PKC isoforms.

ACKNOWLEDGEMENT

This work was supported by the British Heart Foundation (PG/16/94/32393).

CONFLICT OF INTEREST

The authors declare no conflicts of interest.

AUTHOR CONTRIBUTIONS

P.D., L.B., and D.R. carried out the experiments and analysed the data. S.J.F. designed the experiments and wrote the manuscript.

DECLARATION OF TRANSPARENCY AND SCIENTIFIC RIGOUR

This Declaration acknowledges that this paper adheres to the principles for transparent reporting and scientific rigour of preclinical research as stated in the *BJP* guidelines for Design & Analysis, and Immunoblotting and Immunochemistry, and as recommended by funding agencies, publishers, and other organisations engaged with supporting research.

ORCID

Samuel J. Fountain https://orcid.org/0000-0002-6028-0548

REFERENCES

Alexander, S. P. H., Christopoulos, A., Davenport, A. P., Kelly, E., Marrion, N. V., Peters, J. A., … CGTP Collaborators. (2017). The Concise Guide to PHARMACOLOGY 2017/18: G protein-coupled receptors. *British Journal of Pharmacology*, *174*(S1), S17–S129. https://doi.org/10.1111/bph.13878

Alexander, S. P. H., Fabbro, D., Kelly, E., Marrion, N. V., Peters, J. A., Faccenda, E., … CGTP Collaborators. (2017). The Concise Guide to PHARMACOLOGY 2017/18: Enzymes. *British Journal of Pharmacology*, *174*(S1), S272–S359. https://doi.org/10.1111/bph.13877

Alon, R., & Feigelson, S. W. (2012). Chemokine-triggered leukocyte arrest: force-regulated bi-directional integrin activation in quantal adhesive contacts. *Current Opinion in Cell Biology*, *24*, 670–676. https://doi.org/10.1016/j.ceb.2012.06.001

Ashida, N., Arai, H., Yamasaki, M., & Kita, T. (2001). Distinct signaling pathways for MCP-1-dependent integrin activation and chemotaxis. *The Journal of Biological Chemistry*, *276*, 16555–16560. https://doi.org/10.1074/jbc.M009068200

Assani, K., Shrestha, C. L., Robledo-Avila, F., Rajaram, M. V., Partida-Sanchez, S., Schlesinger, L. S., & Kopp, B. T. (2017). Human cystic fibrosis macrophages have defective calcium-dependent protein kinase C activation of the NADPH oxidase, an effect augmented by *Burkholderia cenocepacia*. *Journal of Immunology*, *198*, 1985–1994. https://doi.org/10.4049/jimmunol.1502609

Bartlett, P. J., Metzger, W., Gaspers, L. D., & Thomas, A. P. (2015). Differential regulation of multiple steps in inositol 1,4,5-trisphosphate signaling by protein kinase C shapes hormone-stimulated Ca^{2+} oscillations. *The Journal of Biological Chemistry*, *290*, 18519–18533. https://doi.org/10.1074/jbc.M115.657767

Boring, L., Gosling, J., Cleary, M., & Charo, I. F. (1998). Decreased lesion formation in CCR2−/− mice reveals a role for chemokines in the initiation of atherosclerosis. *Nature*, *394*, 894–897. https://doi.org/10.1038/29788

Campwala, H., Sexton, D. W., Crossman, D. C., & Fountain, S. J. (2014). P2Y(6) receptor inhibition perturbs CCL2-evoked signalling in human monocytic and peripheral blood mononuclear cells. *Journal of Cell Science*, *127*, 4964–4973. https://doi.org/10.1242/jcs.159012

Cronshaw, D. G., Owen, C., Brown, Z., & Ward, S. G. (2004). Activation of phosphoinositide 3-kinases by the CCR4 ligand macrophage-derived chemokine is a dispensable signal for T lymphocyte chemotaxis. *Journal of Immunology*, *172*, 7761–7770. https://doi.org/10.4049/jimmunol.172.12.7761

Curtis, M. J., Alexander, S., Cirino, G., Docherty, J. R., George, C. H., Giembycz, M. A., … Ahluwalia, A. (2018). Experimental design and analysis and their reporting II: updated and simplified guidance for authors and peer reviewers. *British Journal of Pharmacology*, *175*(7), 987–993. https://doi.org/10.1111/bph.14153

Dale, M. M., & Penfield, A. (1987). Comparison of the effects of indomethacin, RHC80267 and R59022 on superoxide production by 1,oleoyl-2, acetyl glycerol and A23187 in human neutrophils. *British Journal of Pharmacology*, *92*, 63–68. https://doi.org/10.1111/j.1476-5381.1987.tb11296.x

de Chaffoy de Courcelles, D., Roevens, P., Van Belle, H., Kennis, L., Somers, Y., & De Clerck, F. (1989). The role of endogenously formed diacylglycerol in the propagation and termination of platelet activation. A biochemical and functional analysis using the novel diacylglycerol kinase inhibitor, R 59 949. *The Journal of Biological Chemistry*, *264*, 3274–3285.

de Wit, R. H., de Munnik, S. M., Leurs, R., Wischer, H. F., & Smit, M. J. (2016). Molecular pharmacology of chemokine receptors. *Methods in Enzymology*, *570*, 457–515. https://doi.org/10.1016/bs.mie.2015.12.002

Drechsler, M., Duchene, J., & Soehnlein, O. (2015). Chemokines control mobilization, recruitment, and fate of monocytes in atherosclerosis. *Arteriosclerosis, Thrombosis, and Vascular Biology*, *35*, 1050–1055. https://doi.org/10.1161/ATVBAHA.114.304649

Dzenko, K. A., Andjelkovic, A. V., Kuziel, W. A., & Pachter, J. S. (2001). The chemokine receptor CCR2 mediates the binding and internalization of monocyte chemoattractant protein-1 along brain microvessels. *The Journal of Neuroscience*, *21*, 9214–9223. https://doi.org/10.1523/JNEUROSCI.21-23-09214.2001

Goekjian, P. G., & Jirousek, M. R. (1999). Protein kinase C in the treatment of disease: Signal transduction pathways, inhibitors, and agents in development. *Current Medicinal Chemistry*, *6*, 877–903.

Griffith, J. W., Sokol, C. L., & Luster, A. D. (2014). Chemokines and chemokine receptors: Positioning cells for host defense and immunity. *Annual Review of Immunology*, *32*, 659–702. https://doi.org/10.1146/annurev-immunol-032713-120145

Gschwendt, M., Dieterich, S., Rennecke, J., Kittstein, W., Mueller, H. J., & Johannes, F. J. (1996). Inhibition of protein kinase C mu by various inhibitors. Differentiation from protein kinase c isoenzymes. *FEBS Letters*, *392*, 77–80. https://doi.org/10.1016/0014-5793(96)00785-5

Gu, L., Okada, Y., Clinton, S. K., Gerard, C., Sukhova, G. K., Libby, P., & Rollins, B. J. (1998). Absence of monocyte chemoattractant protein-1 reduces atherosclerosis in low density lipoprotein receptor-deficient mice. *Molecular Cell*, *2*, 275–281. https://doi.org/10.1016/S1097-2765(00)80139-2

Harding, S. D., Sharman, J. L., Faccenda, E., Southan, C., Pawson, A. J., Ireland, S., … NC-IUPHAR (2018). The IUPHAR/BPS Guide to PHARMACOLOGY in 2018: Updates and expansion to encompass the new guide to IMMUNOPHARMACOLOGY. *Nucleic Acids Research*, *46*, D1091–D1106. https://doi.org/10.1093/nar/gkx1121

Horuk, R. (2009). Chemokine receptor antagonists: Overcoming developmental hurdles. *Nature Reviews. Drug Discovery*, *8*, 23–33. https://doi.org/10.1038/nrd2734

Kantonen, S., Hatton, N., Mahankali, M., Henkels, K. M., Park, H., Cox, D., & Gomez-Cambronero, J. (2011). A novel phospholipase D2-Grb2-WASp heterotrimer regulates leukocyte phagocytosis in a two-step mechanism. *Molecular and Cellular Biology*, *31*, 4524–4537. https://doi.org/10.1128/MCB.05684-11

Korniejewska, A., McKnight, A. J., Johnson, Z., Watson, M. L., & Ward, S. G. (2011). Expression and agonist responsiveness of CXCR3 variants in human T lymphocytes. *Immunology*, *132*, 503–515. https://doi.org/10.1111/j.1365-2567.2010.03384.x

Layhadi, J. A., Turner, J., Crossman, D., & Fountain, S. J. (2018). ATP evokes Ca^{2+} responses and CXCL5 secretion via $P2X_4$ receptor activation in human monocyte-derived macrophages. *Journal of Immunology*, *200*, 1159–1168. https://doi.org/10.4049/jimmunol.1700965

Lee, D., Kim, J., Beste, M. T., Korestzky, G. A., & Hammer, G. L. (2012). Diacylglycerol kinase zeta negatively regulates CXCR4-stimulated T lymphocyte firm arrest to ICAM-1 under shear flow. *Integrative Biology*, *4*, 606–614. https://doi.org/10.1039/c2ib00002d

Lin, Y. F., Leu, S. J., Huang, H. M., & Tsai, Y. H. (2011). Selective activation of specific PKC isoforms dictating the fate of $CD14^+$ monocytes towards differentiation or apoptosis. *Journal of Cellular Physiology*, *226*, 122–131. https://doi.org/10.1002/jcp.22312

Luo, J., Busillo, J. M., Stumm, R., & Benovic, J. L. (2017). G protein-coupled receptor kinase 3 and protein kinase C phosphorylate the distal C-terminal tail of the chemokine receptor CXCR4 and mediate recruitment of β-arrestin. *Molecular Pharmacology*, *91*, 554–566. https://doi.org/10.1124/mol.116.106468

Lutgens, E., Faber, B., Schapira, K., Evelo, C. T., van Haaften, R., Heeneman, S., … Daemen, M. J. (2005). Gene profiling in atherosclerosis reveals a key role for small inducible cytokines: Validation using a novel monocyte chemoattractant protein monoclonal antibody. *Circulation*, *111*, 3443–3452. https://doi.org/10.1161/CIRCULATIONAHA.104.510073

Luther, S. A., Bidgol, A., Hargreaves, D. C., Schmidt, A., Xu, Y., Paniyadi, J., … Cyster, J. G. (2002). Differing activities of homeostatic chemokines CCL19, CCL21, and CXCL12 in lymphocyte and dendritic cell recruitment and lymphoid neogenesis. *Journal of Immunology*, *169*, 424–433. https://doi.org/10.4049/jimmunol.169.1.424

Maus, U., Henning, S., Wenschuh, H., Mayer, K., Seeger, W., & Lohmeyer, J. (2002). Role of endothelial MCP-1 in monocyte adhesion to inflamed human endothelium under physiological flow. *American Journal of Physiology. Heart and Circulatory Physiology*, *283*, H2584–H2591. https://doi.org/10.1152/ajpheart.00349.2002

Micklewright, J. J., Layhadi, J. A., & Fountain, S. J. (2018). P2Y12 receptor modulation of ADP-evoked intracellular Ca^{2+} signalling in THP-1 human monocytic cells. *British Journal of Pharmacology*, *175*, 2483–2491. https://doi.org/10.1111/bph.14218

Nardelli, B., Tiffany, H. L., Bong, G. W., Yourey, P. A., Morahan, D. K., Li, Y., … Alderson, R. F. (1999). Characterization of the signal transduction pathway activated in human monocytes and dendritic cells by MPIF-1, a specific ligand for CC chemokine receptor 1. *Journal of Immunology*, *162*, 435–444.

Rainero, E., Cianflone, C., Porporato, P. E., Chianale, F., Malacame, V., Bettio, V., … Graziani, A. (2014). The diacylglycerol kinase α/atypical PKC/β1 integrin pathway in SDF-1α mammary carcinomainvasiveness. *PLoS ONE*, *9*, e97144. https://doi.org/10.1371/journal.pone.0097144

Reisenberg, M., Singh, P. K., Williams, G., & Doherty, P. (2012). The diacylglycerol lipases: Structure, regulation and roles in and beyond endocannabinoid signalling. *Philosophical Transactions of the Royal Society of London. Series B, Biological Sciences*, *367*, 3264–3275. https://doi.org/10.1098/rstb.2011.0387

Sanjuan, M. A., Pradet-Balade, B., Jones, D. R., Martinez, A. C., Stone, J. C., Garcia-Sanz, J. A., & Mérida, I. (2003). T cell activation in vivo targets diacylglycerol kinase α to the membrane: A novel mechanism for Ras attenuation. *Journal of Immunology*, *170*, 2877–2883. https://doi.org/10.4049/jimmunol.170.6.2877

Schober, A., Manka, D., von Hundleshausen, P., Huo, Y., Hanrath, P., Saremock, I. J., … Weber, C. (2002). Deposition of platelet RANTES triggering monocyte recruitment requires P-selectin and is involved in neointima formation after artery injury. *Circulation*, *106*, 1523–1529. https://doi.org/10.1161/01.CIR.0000028590.02477.6F

Serbina, N. V., & Pamer, E. G. (2006). Monocyte emigration from bone marrow during bacterial infection requires signals mediated by chemokine receptor CCR2. *Nature Immunology*, *7*, 311–317.

Veillard, N. R., Steffens, S., Pelli, G., Lu, B., Kwak, B. R., Gerard, C., … Mach, F. (2005). Differential influence of chemokine receptors CCR2 and CXCR3 in development of atherosclerosis in vivo. *Circulation*, *112*, 870–878. https://doi.org/10.1161/CIRCULATIONAHA.104.520718

Volpe, S., Cameroni, E., Moepps, B., Thelen, S., Apuzzo, T., & Thelen, M. (2012). CCR2 acts as scavenger for CCL2 during monocyte chemotaxis. *PLoS ONE*, *7*, e37208. https://doi.org/10.1371/journal.pone.0037208

Wang, D. L., Wung, B. S., Shyy, Y. J., Lin, C. F., Chao, Y. J., Usami, S., & Chien, S. (1995). Mechanical strain induces monocyte chemotactic protein-1 gene expression in endothelial cells. Effects of mechanical strain on monocyte adhesion to endothelial cells. *Circulation Research*, *77*, 294–302.

Webb, A., Johnson, A., Fortunato, M., Platt, A., Crabbe, T., Christie, M. I., … Jopling, L. A. (2008). Evidence for PI-3K-dependent migration of Th17-polarized cells in response to CCR2 and CCR6 agonists. *Journal of Leukocyte Biology*, *84*, 1202–1212. https://doi.org/10.1189/jlb.0408234

Weber, C., Belge, K. U., von Hundelshausen, P., Draude, G., Steppich, B., Mack, M., … Ziegler-Heitbrock, H. W. L. (2000). Differential chemokine receptor expression and function in human monocyte subpopulations. *Journal of Leukocyte Biology*, *67*, 699–704. https://doi.org/10.1002/jlb.67.5.699

Young, S. H., Rey, O., Sinnett-Smith, J., & Rozengurt, E. (2014). Intracellular Ca^{2+} oscillations generated via the Ca^{2+}-sensing receptor are mediated by negative feedback by PKCα at Thr^{888}. *American Journal of Physiology. Cell Physiology*, *306*, C298–C306. https://doi.org/10.1152/ajpcell.00194.2013

Zernecke, A., & Weber, C. (2010). Chemokines in the vascular inflammatory response of atherosclerosis. *Cardiovascular Research*, *86*, 192–201. https://doi.org/10.1093/cvr/cvp391

Zhang, N., Hodge, D., Rogers, T. J., & Oppenheim, J. J. (2003). Ca^{2+}-independent protein kinase Cs mediate heterologous desensitization of leukocyte chemokine receptors by opioid receptors. *The Journal of Biological Chemistry*, *278*, 12729–12736. https://doi.org/10.1074/jbc.M300430200

SUPPORTING INFORMATION

Additional supporting information may be found online in the Supporting Information section at the end of the article.

How to cite this article: Day P, Burrows L, Richards D, Fountain SJ. Inhibitors of DAG metabolism suppress CCR2 signalling in human monocytes. *Br J Pharmacol*. 2019;176: 2736–2749. https://doi.org/10.1111/bph.14695